



Similarity solution of axisymmetric flow in porous media

L. Li^{a,b,*}, D.A. Lockington^a, M.B. Parlange^c, F. Stagnitti^d, D.-S. Jeng^e,
J.S. Selker^f, A.S. Telyakovskiy^g, D.A. Barry^{b,c}, J.-Y. Parlange^h

^a School of Engineering, The University of Queensland, Brisbane 4072, Australia

^b Centre for Eco-Environmental Modelling, Hohai University, Nanjing 210098, P.R. China

^c École Polytechnique Fédérale de Lausanne (EPFL), School of Architecture, Civil and Environmental Engineering, Ecublens 1015-CH, Switzerland

^d School of Ecology and Environment, Deakin University, P.O. Box 423, Warrnambool, Vic. 3280, Australia

^e Department of Civil Engineering, The University of Sydney, NSW 2006, Australia

^f Bioengineering Department, Oregon State University, Corvallis, OR 13906, USA

^g Department of Mathematics, University of Nevada, Reno, NV 89557-0042, USA

^h Department of Biological and Environmental Engineering, Cornell University, Ithaca, NY 14853-5701, USA

Received 1 June 2004; received in revised form 11 April 2005; accepted 13 April 2005

Abstract

Applications of the axisymmetric Boussinesq equation to groundwater hydrology and reservoir engineering have long been recognised. An archetypal example is invasion by drilling fluid into a permeable bed where there is initially no such fluid present, a circumstance of some importance in the oil industry. It is well known that the governing Boussinesq model can be reduced to a nonlinear ordinary differential equation using a similarity variable, a transformation that is valid for a certain time-dependent flux at the origin. Here, a new analytical approximation is obtained for this case. The new solution, which has a simple form, is demonstrated to be highly accurate.

© 2005 Elsevier Ltd. All rights reserved.

Keywords: Drilling mud invasion; Density-dependent flow; Groundwater pumping; Axisymmetric flow; Boussinesq equation; Sparging

1. Introduction

Boussinesq-type approximations are often used for modelling flow in porous media where sharp interfaces exist and the horizontal component of the flux dominates the vertical component. In groundwater hydrology, where pumping of shallow aquifers is widespread, Boussinesq models are invoked to describe the radial

flow to or from a well (e.g. [1,4,7,8,21]). Similarly, flow in hill slopes (e.g. [9,17,24,26]) and coastal aquifers (e.g. [2,12,15,18,25]) is often modelled using Boussinesq approaches. Because these models are based on a nonlinear governing equation, linearisation is a feature of many solutions (e.g. [3,6,13,19,28,29]). That is, the practical applications of the solution to the Boussinesq equation have long been recognised.

Axisymmetric flow regimes are a feature of groundwater systems subject to pumping, as mentioned above in terms of groundwater utilisation. Air sparging in porous media also gives rise to flow with dominant horizontal components and a sharp interface between the injected and resident fluids (e.g. [20,23,27]). Another example involving pumping is invasion of drilling fluid into a permeable bed. For the problem of drilling fluid

* Corresponding author. Tel.: +61 7 3365 3911; fax: +61 7 3365 4599.

E-mail addresses: l.li@uq.edu.au (L. Li), d.lockington@uq.edu.au (D.A. Lockington), marc.parlange@epfl.ch (M.B. Parlange), frankst@deakin.edu.au (F. Stagnitti), d.jeng@civil.usyd.edu.au (D.-S. Jeng), john.selker@orst.edu (J.S. Selker), alekseyt@unr.edu (A.S. Telyakovskiy), andrew.barry@epfl.ch (D.A. Barry), jp58@cornell.edu (J.-Y. Parlange).

invasion, Barenblatt’s work in the 1950s [see references in 5] using self-similar solutions in particular has been widely used. Dussan and Auzeais [11] have discussed the problem in great detail in the context of oil drilling where they assumed a power-law flux into the porous medium exists.

The purpose of this note is to re-examine similarity solutions to the axisymmetric Boussinesq model, building on Barenblatt’s [5] approach, with the aim of obtaining improved approximate solutions for axisymmetric flow. This similarity-variable approach was also used by Dussan and Auzeais [11], and their results appear as a special case of the results presented below. In order to motivate the theory, we present the problem of drilling mud invasion as a significant process where the axisymmetric Boussinesq model is appropriate. Other flow processes could be modelled similarly.

2. Drilling mud invasion

Doll [10] provided an early investigation of drilling mud invasion into a permeable aquifer. The problem is discussed in detail by Doll [10], Dussan and Auzeais [11] and Ramakrishnan and Wilkinson [22]; only a brief discussion based on these papers is presented here.

During well drilling, filtrate (drilling mud) invades the porous medium as it is kept at a higher pressure than the formation fluid. This is to prevent escape of formation fluid during drilling. Mud cake builds up on the wall of the well, restricting the mud invasion of the formation. Indeed, the mud cake controls entry of the filtrate due to its relatively low (compared with the formation) permeability.

Fig. 1 provides a schematic diagram of the mud invasion into a permeable layer bounded above and below by impermeable layers. Mud cake builds up on the well wall, leading to essentially horizontal discharge into the formation. When filtrate enters the formation, it moves

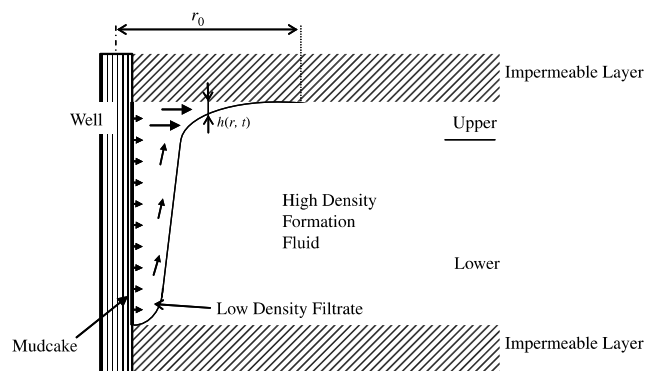


Fig. 1. Schematic depiction of drilling fluid (filtrate) penetrating a homogeneous confined porous medium. In the upper region (marked) the flow is predominantly horizontal. In this region, the interface position obeys the radial Boussinesq equation.

horizontally due to the positive pressure difference between the well and the formation fluid, and vertically due to buoyancy (filtrate is typically much less dense than formation fluid). As shown in Fig. 1, this leads to a profile that is very narrow at the bottom of the permeable layer, while expanding at its top. At the top of the permeable layer, the filtrate flux is essentially horizontal. For relatively large buoyancy contrasts, Dussan and Auzeais [10] show that the interface position above the impermeable base within the upper layer is described by the radial Boussinesq equation, presented below.

3. Theory

The dynamic movement of the interface between two fluids (for instance air and water in the case of a pumping well) can in certain circumstances be described by the Boussinesq equation (e.g., see [5])

$$\theta_s \frac{\partial h}{\partial t} - \frac{K_s}{r} \frac{\partial}{\partial r} \left(rh \frac{\partial h}{\partial r} \right) = 0, \quad (1)$$

where $h(r, t)$ is the interface position as defined in Fig. 1 (relative to the upper impermeable boundary; i.e., the thickness of the upper filtrate layer), t the time, r the distance from the line source, K_s the saturated conductivity and θ_s the porosity. We look for a self-similar solution following [5]. In [5], a power-law flux (where the power is related to the parameter α) at the origin is assumed and dimensional analysis of Eq. (1) allows the deduction that h should be of the form

$$h = Mt^{\frac{\alpha-1}{2}} f(\eta) \quad (2)$$

with

$$r = \eta Nt^{\frac{\alpha+1}{4}}. \quad (3)$$

Note that Eq. (2) gives $h(r, 0) = 0$. Since f will be determined below, without loss of generality we relate the constants M and N by

$$MK_s = N^2 \theta_s \quad (4)$$

and define N in terms of the front position r_0 where $h = 0$, so that [5]

$$r_0 = Nt^{\frac{\alpha+1}{4}}, \quad (5)$$

which imposes the condition

$$f(1) = 0. \quad (6)$$

Physically, Eq. (5) means that initially the front is at the origin of r . Eq. (1) gives the differential equation for $f(\eta)$ as [5]:

$$\left(\frac{\alpha+1}{4} \right) \eta \frac{df}{d\eta} - \left(\frac{\alpha-1}{2} \right) f + \frac{1}{\eta} \frac{d}{d\eta} \left(\eta f \frac{df}{d\eta} \right) = 0. \quad (7)$$

Eq. (7) does not admit an exact solution. Below, we will seek an improved approximation to f . Note that α is

undefined at this stage although as mentioned in [5] it is related to the flux at the origin of r . That is, it is determined by imposition of the boundary condition at the origin of the co-ordinate system. The boundary condition is that the flux, q , is known at $r = 0$, with

$$q = -K_s 2\pi r h \frac{\partial h}{\partial r} \quad \text{at } r = 0 \quad (8)$$

or from Eqs. (2) and (3)

$$q = -K_s 2\pi M^2 t^{\alpha-1} \left[\eta f(\eta) \frac{df}{d\eta} \right]_{\eta=0}. \quad (9)$$

Thus, we observe that α controls the flux at the origin. We see that $\int_0^t q d\bar{t}$ must be finite and thus $\alpha > 0$. Dussan and Auzeais [11] show that the cases of $\alpha = 1, 2$ have special physical significance for the filtrate invasion problem described above; $\alpha = 1$ describes a constant flux condition whereas $\alpha = 2$ corresponds to a flux that increases linearly with time.

Integration of Eq. (1) yields the overall conservation of mass

$$q = 2\pi\theta_s \int_0^{r_0} r \frac{\partial h}{\partial t} dr \quad (10)$$

or, from Eqs. (2)–(4) and (9),

$$\left[\eta f(\eta) \frac{df}{d\eta} \right]_{\eta=0} = -\alpha \int_0^1 f(\eta) \eta d\eta. \quad (11)$$

Eq. (11) can also be obtained directly by integration of Eq. (7) over η between zero and one recognising that the flux is zero at $r = r_0$ i.e., $\eta = 1$. Integration of Eq. (7) between η and one gives

$$\frac{df}{d\eta} + \left(\frac{\alpha + 1}{4} \right) \eta = -\frac{\alpha}{f\eta} \int_{\eta}^1 f \bar{\eta} d\bar{\eta}. \quad (12)$$

In particular at $\eta = 1$ where $f = 0$ Eq. (12) shows that

$$\frac{df}{d\eta} = -\frac{1 + \alpha}{4} \quad \text{at } \eta = 1. \quad (13)$$

Eqs. (6) and (13) can be used to integrate Eq. (7) numerically using for example the fourth-order Runge–Kutta method without any difficulty as done by Dussan and Auzeais [11]. These authors also derived an expansion of the solution valid near $\eta = 1$, i.e.

$$f \sim \left(\frac{\alpha + 1}{4} \right) (1 - \eta) + \left(\frac{\alpha - 1}{8} \right) (1 - \eta)^2 + \left(\frac{\alpha + 3}{\alpha + 1} \right) \frac{\alpha}{36} (1 - \eta)^3 + \dots \quad (14)$$

3.1. Estimate of the front position

An important parameter comes from the first moment of f , i.e., $\int_0^1 f \eta d\eta$. As we shall see shortly, it is related, for instance, to the position of the front, r_0

From Eqs. (9) and (11) we have, for the cumulative flux:

$$\int_0^t q d\bar{t} = Ct^\alpha, \quad (15)$$

where C is the constant

$$C = K_s 2\pi M^2 \int_0^1 f(\eta) \eta d\eta \quad (16)$$

and the front position, r_0 is, from Eqs. (4), (5) and (16),

$$r_0^4 = \frac{K_s t^{\alpha+1} C}{2\pi\theta_s^2 \int_0^1 f \eta d\eta}, \quad (17)$$

yielding r_0 as a function of α once $\int_0^1 f \eta d\eta$ is known. Several estimates of this integral are presented below.

Eq. (12) has a convenient form to discuss the properties of the solution. For instance it shows that as $\eta \rightarrow 0$:

$$f^2 \approx -\alpha \ln(\eta^2) \int_0^1 f \eta d\eta. \quad (18)$$

Also, for α small an expansion is obtained easily by iteration as

$$f \approx \frac{1}{8} (1 - \eta^2) - \frac{\alpha}{8} \ln(\eta^2) - \frac{\alpha^2}{4} \left[\ln(\eta^2) + \frac{1}{4} \ln^2(\eta^2) + \text{dilog}(\eta^2) \right] + \dots, \quad (19)$$

where dilog is the dilogarithm function [14]. Eq. (19) is consistent with Eq. (14) for the first two terms. The first two terms of Eq. (19) lead to the first estimate:

$$\int_0^1 f \eta d\eta \approx \frac{1}{32} + \frac{\alpha}{16}. \quad (20)$$

A very similar result can be obtained from the first two terms of Eq. (14), $\frac{1}{32} + \frac{3\alpha}{96}$. Surprisingly, Eq. (20) leads to an estimate of $\int_0^1 f \eta d\eta$ numerically close to that of Dussan and Auzeais [11] for all α 's. This supports the notion that Eq. (19) can be used in an iterative process. The three terms in Eq. (19) then give for the first moment of f :

$$\int_0^1 f \eta d\eta \approx \frac{1}{32} + \frac{\alpha}{16} - \frac{\alpha^2}{8} \left(\frac{\pi^2}{6} - \frac{3}{2} \right), \quad (21)$$

which reduces to Eq. (20) when the $O(\alpha^2)$ term is dropped.

Eq. (21) is valid for α small only, as noted above. However, observe from the large α limit of Eq. (7) that f and thus $\int_0^1 f \eta d\eta$ are proportional to α as $\alpha \rightarrow \infty$; thus it is natural to express $\int_0^1 f \eta d\eta$ as a continued-fraction approximation

$$\int_0^1 f \eta d\eta \approx \frac{1}{32} + \frac{\alpha}{16} \left(\frac{1 + A\alpha}{1 + B\alpha} \right), \quad (22)$$

where A and B are two constants that are relatively close such that Eq. (20) is approximately satisfied. From Eq. (21) we retrieve the condition

$$B - A = \frac{\pi^2}{3} - 3 \approx 0.29. \quad (23)$$

An additional equation is needed to obtain A and B and thus we seek an integral condition since our approximation is to be applicable for all $\alpha > 0$. We can, for instance, multiply Eq. (12) by $f\eta - \eta^2$ and by integration over η from zero to one, obtain the following results for various terms of Eq. (12):

Term 1 on the left-hand side of Eq. (12)

$$\begin{aligned} \int_0^1 f\eta \frac{df}{d\eta} d\eta^2 &= \int_0^1 \eta^2 \frac{df^2}{d\eta^2} d\eta^2 = \eta^2 f^2 \Big|_0^1 - \int_0^1 f^2 d\eta^2 \\ &= - \int_0^1 f^2 d\eta^2. \end{aligned} \quad (24a)$$

Term 2 on the left-hand side of Eq. (12)

$$\int_0^1 \left(\frac{1+\alpha}{4}\right) \eta f \eta d\eta^2 = \left(\frac{1+\alpha}{4}\right) \int_0^1 f \eta^2 d\eta^2. \quad (24b)$$

Term on the right-hand side of Eq. (12)

$$\begin{aligned} -\alpha \int_0^1 \int_{\eta}^1 f(\bar{\eta}) \bar{\eta} d\bar{\eta} d\eta^2 &= -\frac{\alpha}{2} \int_0^1 \int_{\eta}^1 f(\bar{\eta}) d\bar{\eta}^2 d\eta^2 \\ &= -\frac{\alpha}{2} \int_0^1 f(\bar{\eta}) \left[\int_0^{\bar{\eta}} d\eta^2 \right] d\bar{\eta}^2 \\ &= -\frac{\alpha}{2} \int_0^1 f \eta^2 d\eta^2. \end{aligned} \quad (24c)$$

Combining Eqs. (24a)–(24c) gives

$$\int_0^1 f d\eta^2 = \frac{4}{1+3\alpha} \int_0^1 f^2 d\eta^2 + \int_0^1 (1-\eta^2) f d\eta^2. \quad (24d)$$

We can use an expansion of f^2 to order $(1-\eta^2)^{m+1}$ and to order $(1-\eta^2)^m$ in the right-hand side of Eq. (24d) to obtain a better estimate of the integral on the left-hand side. To calculate the integral directly with the same order of accuracy would have required knowledge of f to order $(1-\eta^2)^{m+1}$. Note that m is a non-negative integer. For this reason, Eq. (24d) is an appropriate expression to calculate $\int_0^1 f(\eta) d\eta^2$ approximately.

The first two terms of Eq. (19) yield the approximation given in Eq. (20), which is already a reasonable approximation. For the same starting point, use of Eq. (24d) should yield a better approximation. Doing so we obtain at once,

$$\int_0^1 f\eta d\eta \approx \frac{1}{32} + \frac{\alpha}{16} \left(\frac{1 + \frac{13}{4}\alpha}{1 + 3\alpha} \right). \quad (25)$$

We should expect this estimate to be too large as f^2 used in Eq. (24d) behaves like $\ln^2(\eta^2)$ for the $O(\alpha^2)$ term, whereas Eq. (18) shows that it should behave like $\ln(\eta^2)$

only. Dropping this α^2 term yields another approximation:

$$\int_0^1 f\eta d\eta \approx \frac{1}{32} + \frac{\alpha}{16} \frac{1 + \frac{9}{4}\alpha}{1 + 3\alpha}. \quad (26)$$

This expression underestimates the first moment because the coefficient of the $\ln(\eta^2)$ term as $\eta \rightarrow \infty$ is $\frac{\alpha}{32}$ and we know from Eq. (18) that it should be larger. Eq. (23) confirms that the estimate of Eq. (26) is too low while that of Eq. (25) is too high. $B - A$ in Eq. (26) is too large and too low in Eq. (25). Thus, the geometric average of the two terms,

$$\int_0^1 f\eta d\eta = \frac{1}{32} + \frac{\alpha}{16} \frac{1 + \frac{3\sqrt{13}\alpha}{4}}{1 + 3\alpha}, \quad (27)$$

should be quite accurate as $3 - \frac{3\sqrt{13}}{4} \approx 0.296$ is very close to the low α limit of Eq. (23), i.e. $\frac{\pi^2}{3} - 3 \approx 0.290$. An obvious alternative to Eq. (27) is to keep $B = 3$ as suggested by both Eqs. (25) and (26) and calculate A from Eq. (23), giving,

$$\int_0^1 f\eta d\eta = \frac{1}{32} + \frac{\alpha}{16} \frac{1 + \left(6 - \frac{\pi^2}{3}\right)\alpha}{1 + 3\alpha}, \quad (28)$$

which is indeed very slightly more accurate than Eq. (27), as will be checked later.

3.2. Improved approximations for f

We are now going to find new, accurate approximations for $f(\eta)$, which, we recall, is key to the solution for h as shown by Eq. (2). As we have seen already in the previous section, η^2 is a more natural variable than η due to the axisymmetric nature of the problem. It is also more convenient to operate with f^2 because of Eq. (18). Eq. (14) then, up to terms of $O(\alpha^2)$, becomes (cf. [16]):

$$\begin{aligned} f^2 &= \left(\frac{\alpha+1}{8}\right)^2 (1-\eta^2)^2 + \frac{\alpha(\alpha+1)}{64} (1-\eta^2)^3 \\ &\quad + \frac{\alpha(29\alpha+24)}{2304} (1-\eta^2)^4 + \dots, \end{aligned} \quad (29)$$

valid for $1-\eta^2$ small, whereas for η small the solution has a logarithmic singularity given by Eq. (18). Note that the limit of $\alpha = 0$ from Eq. (29) reduces to the exact solution $f = (1-\eta^2)/8$, like Eq. (14). The aim is to produce a uniform approximation valid for all η . The Taylor expansion in Eq. (29) is quite straightforward and additional terms can be obtained without difficulty. However, we shall consider only three terms to match the three-term expansion of Dussan and Auzerais [11]. We shall check later that it provides sufficient accuracy for any purpose. In general, though, we can rewrite Eq. (29) as,

$$f_1^2 = \sum_{n=1}^p Z_n (1 - \eta^2)^{n+1}, \quad (30)$$

where the Z_n 's are to be appropriately determined and the upper limit of the summation, p , could be infinite. In the truncated expansion of Eq. (29) we set $p = 3$ with

$$Z_1 = \left(\frac{\alpha+1}{8}\right)^2; \quad Z_2 = \frac{\alpha(\alpha+1)}{64} \quad \text{and} \quad Z_3 = \frac{\alpha(29\alpha+24)}{2304}. \quad (31)$$

We use the notation f_1 in Eq. (30) as a reminder that the expansion is valid near $\eta^2 = 1$. Near $\eta^2 = 0$ the solution must satisfy Eq. (19), so we combine the two expressions to provide a new approximation

$$f^2 \approx f_1^2 - \alpha \left[\ln(\eta^2) + \sum_{n=1}^{m+1} \frac{(1 - \eta^2)^n}{n} \right] \int_0^1 f \eta d\eta. \quad (32)$$

Since $\sum_{n=1}^{m+1} \frac{(1 - \eta^2)^n}{n}$ is the expansion of $-\ln(\eta^2)$ near $\eta^2 = 1$, the expression in Eq. (32) is valid to $O(1 - \eta^2)^{m+1}$ whatever the value of m . Also, by construction Eq. (32) satisfies Eq. (18) near $\eta^2 = 0$ for any m . Thus, Eq. (32) provides a uniform approximation. Of course, we now have to check its accuracy and its apparent convergence as m increases. This is done below.

4. Discussion

To apply Eq. (32) we require the value for $\int_0^1 f d\eta^2$ given by, for instance, Eq. (28). We could also use an iterative technique by choosing some value for this parameter, calculate f^2 from Eq. (32) and calculate $\int_0^1 f d\eta^2$ from this estimate and use this estimate to reiterate until convergence is obtained. The iterated values in Table 1 were so obtained. However, they are given here only as a check of convergence. It is clear that this iterative calculation of $\int_0^1 f d\eta^2$ is numerical and thus largely defeats the purpose of our study, which is to provide a fully analytical solution, especially since the numerical solution of the original problem based on, for example the finite-difference method, is straightforward and iteration provides no significant improvement.

Table 1, in addition to the iterated values, provides $\int_0^1 \frac{f d\eta^2}{1+\alpha}$ obtained exactly (numerically) and analytical estimates from Eqs. (27) and (28) for $\alpha = 1/2, 1, 3/2, 2, 5, \infty$. Note we divided the result by $\alpha + 1$ to obtain a finite result when $\alpha \rightarrow \infty$. In this limit, the power-law flux at the origin reduces to an exponential flux, as shown in Appendix A. Note, also, that for $\alpha = 0$, the analytical result $f = \frac{1-\eta^2}{8}$ is the exact result as provided by our procedure.

Fig. 2 shows the details of the profiles, $\frac{f}{\alpha+1}$, obtained numerically and analytically for $m = 1, 2$ and 3, using

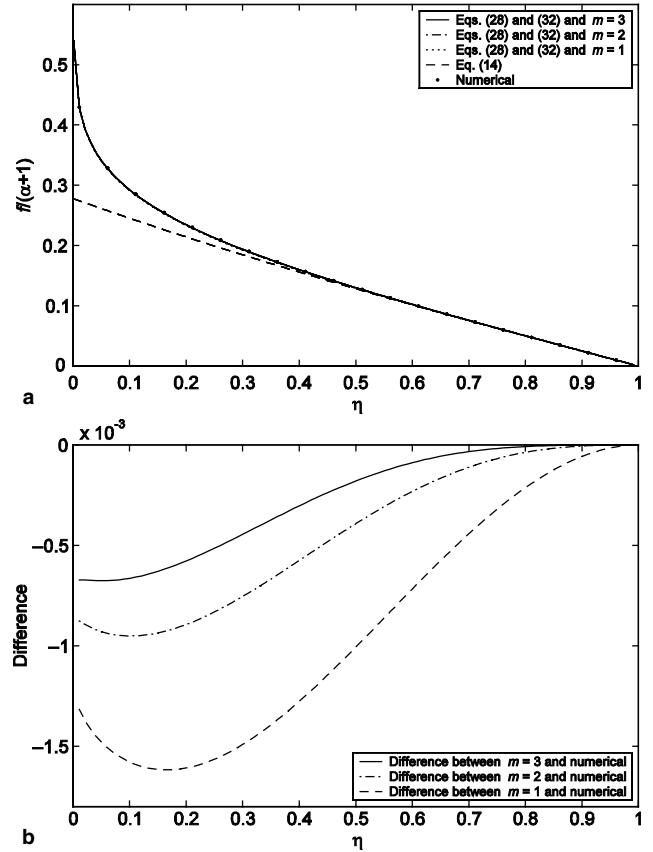


Fig. 2. (a) Profiles of $\frac{f}{\alpha+1}$ versus η obtained numerically and analytically using Eqs. (28) and (32) ($m = 1, 2$ and 3) and also Eq. (14) keeping 1, 2 or 3 terms, for $\alpha = 1$. (b) Absolute differences between the analytical solutions and the numerical prediction.

Table 1
Calculated values of $\int_0^1 \frac{f d\eta^2}{1+\alpha}$ using different methods

	$\alpha = 0.5$	$\alpha = 1$	$\alpha = 1.5$	$\alpha = 2$	$\alpha = 5$	$\alpha \rightarrow \infty^a$
Eq. (27)	0.0790	0.0858	0.0896	0.0920	0.0978	0.1036
Eq. (28)	0.0810	0.0892	0.0940	0.0972	0.1052	0.1130
Evaluation of the integral based on the iterated solution of f , i.e., Eq. (32) with $m = 3$, in which Eq. (27) is used as a first approximation	0.0806	0.0888	0.0936	0.0968	0.1046	0.1118
Evaluation of the integral based on the iterated solution of f , i.e., Eq. (32) with $m = 3$, in which Eq. (28) is used as a first approximation	0.0808	0.0892	0.0942	0.0974	0.1056	0.1124
Numerical solution	0.0810	0.0894	0.0942	0.0973	0.1051	0.1126

^a This limit corresponds to an exponential flux at the origin (see Appendix A).

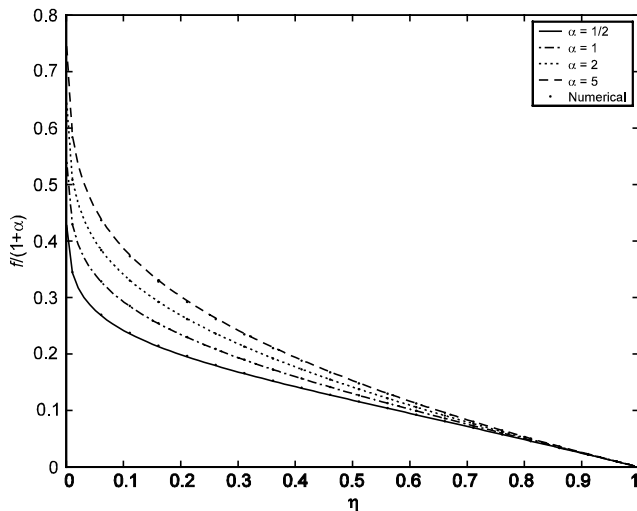


Fig. 3. Profiles of $\frac{f}{1+\alpha}$ versus η obtained numerically, and using Eqs. (28) and (32) ($m = 3$) for different values of α .

Eqs. (28) and (32) and also Eq. (14) keeping 1, 2 or 3 terms. We show the results for $\alpha = 1$ only. Other values of α give similar results, i.e., there is little difference between the numerical results and the analytical approximation given in Eq. (32). The calculations have been given for $m = 1, 2$ and 3 and we notice the slight improvement as m increases. Also (as shown in Table 1), the iterated value (of the first moment of f) provides only slight improvement over the analytical result, i.e., Eqs. (32) and (28). Thus, the latter is all that is required and is remarkably accurate, justifying our procedure. Even the simple result for $m = 1$ is quite accurate and as shown in Fig. 2a there is no noticeable difference between the analytical approximations for $m = 1, 2$ and 3, and the exact result. More detail on the absolute differences is shown in Fig. 2b. As expected, Eq. (14) is far less accurate. Finally, Fig. 3 gives the profiles for several α 's and $m = 3$. We see that the accuracy of the prediction is very satisfactory for all cases.

5. Conclusions

By combining a straightforward Taylor expansion with the known logarithmic singularity at $\eta = 0$ we obtained a very accurate solution to an axisymmetric Boussinesq problem, viz. one where the flux at the origin varies with time to a power parameterised by α . The simple case keeps only the first term in the expansion, and provides surprisingly accurate results. Adding the second and third terms provides even greater accuracy. The crucial step underlying these results is that the first moment $\int_0^1 f \eta d\eta$ appearing in the right-hand side of the approximation is estimated very accurately (which also provides an excellent estimate of the front position, see Eq. (17)).

The procedure followed here seems quite general and might possibly be used in other problems when a Taylor expansion is obtainable at one point and a singularity is present at another point. Although there is similarity with a standard boundary-layer approach we do not require a small parameter. In spite of its apparent generality we were not able to find other examples where this technique has been used.

The theory presented is applicable to situations where predominantly horizontal flow of one fluid displacing another is involved, influent flux obeys a power law and the interface mixing between the two fluids is relatively small. The example of drilling mud fluid given earlier fits this description. In that case, a vertical flow region driven by the buoyancy contrast is overlain by a region where predominantly horizontal flow occurs at the top of the confined aquifer. The original analysis of Doll [10] was revisited by Dussan and Auzerais [11] where it was shown that the locations of these regions could be estimated. Nonetheless, the theory presented here is clearly most relevant to the leading edge of the horizontal intrusion, e.g., locating the position of the front.

Acknowledgements

The authors are grateful for the support from Australian Research Council Discovery Grant (2003-2005) #DP0343443.

Appendix A. Limit of large α

Here we show that the large α limit corresponds to the exponential flux at the origin [5]. First, we note that Eq. (7) can be rewritten using the transformation $g = (1 + \alpha)f$:

$$\frac{\eta}{2} \frac{dg}{d\eta} - \left(\frac{\alpha - 1}{\alpha + 1}\right)g + \frac{1}{\eta} \frac{d}{d\eta} \left(\eta \frac{dg^2}{d\eta} \right) = 0. \quad (A1)$$

Now, consider the solution to Eq. (1) using the transformations:

$$h = A \exp\left(\frac{kt}{2}\right)g(\eta) \quad (A2)$$

with

$$r = \eta N \exp\left(\frac{kt}{4}\right). \quad (A3)$$

where

$$A^2 = \frac{N^2 k \theta_s}{K_s}. \quad (A4)$$

Then, Eq. (1) becomes

$$\frac{\eta}{2} \frac{dg}{d\eta} - g + \frac{1}{\eta} \frac{d}{d\eta} \left(\eta \frac{dg^2}{d\eta} \right) = 0. \quad (A5)$$

Eq. (A1) reduces to Eq. (A5) in the limit of $\alpha \rightarrow \infty$. Substitution of the transformations in Eqs. (A2) and (A3) into Eq. (8) shows that for this case the flux at the origin is proportional to $\exp(kt)$. Thus, the large α power-law flux is in the limit an exponential flux.

References

- [1] Aravin VI, Numerov SN. Theory of fluid flow in undeformable porous media. Isr Program for Science Translation Jerusalem; 1965.
- [2] Baird AJ, Mason T, Horn DP. Validation of a Boussinesq model of beach ground water behaviour. *Mar Geol* 1998;48:55–69.
- [3] Barry DA, Barry SJ, Parlange J-Y. Capillarity correction to periodic solutions of the shallow flow approximation. Mixing processes in estuaries and coastal seas. In: Pattiaratchi CB, editors, Coastal and estuarine studies, vol. 50. Washington (DC): American Geophysics Union; 1996. p. 496–510.
- [4] Bear J. Dynamics of fluids in porous media. New York: American Elsevier; 1972.
- [5] Barenblatt GI, Entov VM, Ryzhik VM. Theory of fluid flows through natural rocks. Dordrecht: Kluwer; 1990.
- [6] Brutsaert W. The unit response of groundwater outflow from a hillslope. *Water Resour Res* 1994;30:2759–63.
- [7] Childs E. Drainage of groundwater resting on a sloping bed. *Water Resour Res* 1971;7:1256–63.
- [8] Dagan G. Second order theory of shallow free surface flow in porous media. *Q J Mech Appl Math* 1967;20:517–26.
- [9] Daly E, Porporato A. A note on groundwater flow along a hillslope. *Water Resour Res* 2004;40.
- [10] Doll HG. Filtrate invasion in highly permeable sands. *Petrol Eng* 1955:B53–66.
- [11] Dussan EB, Auzerais FM. Buoyancy-induced flow in porous-media generated near a drilled oil-well. 1. The accumulation of filtrate at a horizontal impermeable boundary. *J Fluid Mech* 1993;254:283–311.
- [12] Jeng DS, Li L, Barry DA. Analytical solution for tidal propagation in a coupled semi-confined/phreatic coastal aquifer. *Adv Water Resour* 2002;25:577–84.
- [13] Kim DJ, Ann MJ. Analytical solutions of water table variation in a horizontal unconfined aquifer: Constant recharge and bounded by parallel streams. *Hydrol Proc* 2001;15:2691–9.
- [14] Lewin L. Polylogarithms and associated functions. North Holland: Amsterdam; 1981.
- [15] Li L, Dong P, Barry DA. Tide-induced water table fluctuations in coastal aquifers bounded by rhythmic shorelines. *ASCE J Hydraul Eng* 2002;128:925–33.
- [16] Lockington DA, Parlange J-Y, Parlange MB, Selker J. Similarity solution of the Boussinesq equation. *Adv Water Resour* 2000;23:725–9.
- [17] Mizumura K. Drought flow from hillslope. *ASCE J Hydrol Eng* 2002;7:109–15.
- [18] Nielsen P, Aseervatham R, Fenton JD, Perrochet P. Groundwater waves in aquifers of intermediate depths. *Adv Water Resour* 1997;20:37–43.
- [19] Pauwels VRN, Verhoest NEC, De Troch FP. A metahillslope model based on an analytical solution to a linearized Boussinesq equation for temporally variable recharge rates. *Water Resour Res* 2002;38.
- [20] Peterson JW, Murray KS, Tulu YI, Peuler BD, Wilkens DA. Air-flow geometry in air sparging of fine-grained sands. *Hydrogeol J* 2001;9:168–76.
- [21] Polubarinova-Kochina PYa. Theory of groundwater movement. Princeton (NJ): Princeton University Press; 1962.
- [22] Ramakrishnan TS, Wilkinson DJ. Formation producibility and fractional flow curves from radial resistivity variation caused by drilling fluid invasion. *Phys Fluids* 1997;9:833–44.
- [23] Reddy KR, Adams JA. Effects of soil heterogeneity on airflow patterns and hydrocarbon removal during in situ air sparging. *ASCE J Geotech Geoenviron Eng* 2001;127:234–47.
- [24] Stagnitti F, Li L, Parlange J-Y, Brutsaert W, Lockington DA, Steenhuis TS, et al. Drying front in a sloping aquifer: Nonlinear effects. *Water Resour Res* 2004;40.
- [25] Teo HT, Jeng DS, Seymour BR, Barry DA, Li L. A new analytical solution for water table fluctuations in coastal aquifers with sloping beaches. *Adv Water Resour* 2003;26:1239–47.
- [26] Upadhyaya A, Chauhan HS. Falling water tables in horizontal/sloping aquifer. *ASCE J Irrigat Drain Eng* 2001;127:378–84.
- [27] van Dijke MIJ, van der Zee SEATM. Modeling of air sparging in a layered soil: Numerical and analytical approximations. *Water Resour Res* 1998;34:341–53.
- [28] Verhoest NEC, Troch PA. Some analytical solutions of the linearized Boussinesq equation with recharge for a sloping aquifer. *Water Resour Res* 2000;36:793–800.
- [29] Verhoest NEC, Troch PA. Correction to “Some analytical solutions of the linearized Boussinesq equation with recharge for a sloping aquifer”. *Water Resour Res* 2000;36:1989.